Invited Paper

Efficiency enhancement of GaN-based LED using nanotechnology

C.H. Chiu, M.A. Tsai, Peichen Yu, and H.C. Kuo

Department of Photonics and Institute of Electro-Optical Engineering, National Chiao Tung University, Hsinchu 30010, Taiwan

ABSTRACT

We had demonstrated several novel methods to improve the luminescence efficiency of the GaN-based light emitting diodes (LEDs). The high-aspect-ratio GaN nanorods, formed by spun nano-spheres and inductively coupled plasma (ICP) etching, contributed to an enhancement in light output power and better light directionality. Nevertheless, the etching process would affect the electrical properties. We then attempt to rough the surface by synthesizing ZnO nanorods in liquid solution at room temperature. The LEDs with ZnO nanorods enjoyed high extraction efficiency and comparable electric performance than that without nanorods. At third part, we fabricate a high efficiency GaN-based LED by regrowth on SiO2 nanorod patterned sapphire substrate. It could improve the light extraction and internal efficiencies simultaneously.

Keywords: GaN & ZnO nanorods, light emitting diodes, nanorod-array patterned sapphire substrate

1. INTRODUCTION

For the past decade, gallium nitride-based light emitting diodes (GaN-based LEDs) have been widely used in various applications such as back- lighting source in display systems, traffic signals, outdoor displays due to the widely tunable wavelength from ultraviolet to blue/green[1]. Most importantly, they have the potential to replace incandescent or fluorescent mercury (Hg) and xenon (Xe) lamps for general lighting devices. To achieve this purpose, the external quantum efficiency (EQE) of LEDs should be further improved.

Basically, the EQE could be viewed as the product of extraction efficiency and internal quantum efficiency (IQE). Regarding to the extraction efficiency, because of the large refraction index difference between GaN (n_{GaN}=2.5) and air (n_{air}=1), the critical angle of light extraction is about 23°. It results in only few percent of generated light could be extracted from the surface and mainly limits the extraction efficiency. To enhance the extraction efficiency, several works, including surface roughening,[2] inclined sidewalls,[3] use of photonic crystals,[4] and diffused mirror techniques[5] have been developed. Moreover, one problem associated with conventional GaN-based LEDs is the poor thermal conductivity of the sapphire substrate. A GaN-based vertical LED combined laser lift-off (LLO) technique and wafer-bonded to another substrate with good thermal conductivity was therefore proposed for high power chips. Compared with lateral injection (conventional) LEDs fabricated on sapphire substrates, vertical LEDs behaved many advantages, such as better current injection, excellent heat dissipation, enhanced reliability with respect to electrostatic discharge, etc.

For the IQE studies, it has been shown that the epitaxial lateral overgrowth (ELO) method with a microscale SiN_x or SiO_x patterned mask on as-grown GaN seed crystals can effectively reduce the threading dislocation density (TDD)[6] and improve the IQE as well. However, the requirements of the two-step growth procedure and a sufficient thickness for GaN coalescence are costly and time consuming. Moreover, high quality GaN-based LEDs have been demonstrated on a microscale patterned sapphire substrate (PSS) by wet etching,[7] where the microscale patterns served as a template for the ELO of GaN and the scattering centers for the guided light. Both the epitaxial crystal quality and the light extraction efficiency were improved. It is then reasonable to nano down the PSS structures into nanoscale. So, recently, the metal–organic chemical vapor deposition (MOCVD) growth of InGaN/GaN LEDs on the nanoscale PSS has been studied and the comparison between nano and micro scale PSS was also reported.[8]

Therefore, this article was composed by three main parts: the first is extraction efficiency enhancement by fabricating high-aspect-ratio GaN nanorod arrays on vertical LED by inductively coupled plasma (ICP) etching; the second part is synthesizing ZnO nanorod arrays on vertical LED, and the third part is regrowth LEDs on SiO_2 nanorod-array PSS.

Photonics and Optoelectronics Meetings (POEM) 2009: Solar Cells, Solid State Lighting, and Information Display Technologies, edited by Michael Grätzel, Hiroshi Amano, Chin Hsin Chen, Changqing Chen, Peng Wang, Proc. of SPIE Vol. 7518, 75180A · © 2009 SPIE · CCC code: 0277-786X/09/$18 · doi: 10.1117/12.843671

2. HIGH-ASPECT-RATIO GAN NANOROD ON VERTICAL LED

We first demonstrate a high efficiency vertical LED with high-aspect-ratio GaN nanorod on the surface. Traditionally, the conventional LED has a view angle about 120°, which is not preferable for applications such as mobile phone cameras, pocket lamps, and vehicle head lamps. Hence, it is essential to develop high-efficiency LEDs with good directional radiation profiles for next-generation lighting devices. However, some of the proposed techniques could deteriorate the electrical properties of conventional LEDs due to the thin p-GaN top layer, limiting the depth of surface textures to 200 nm.

In this part, we proposed a vertical LED structure, where fabricating nanorod arrays with heights over 1 μm is possible.[9] The fabrication of vertical LEDs, which combines wafer bonding and laser lift-off (LLO) techniques, results in a thick n-GaN top layer, providing an excellent platform to fabricate high-aspect-ratio nanorod arrays. The nanorod arrays are patterned by uniformly spun silica spheres, followed by ICP. The technique is relatively cost-effective for mass production, compared to that involving electron-beam lithography.[10] The fabricated nanorods resemble cone structures, which not only provide an omnidirectional escaping zone for photons,[11] but also serve as wave-guiding channels for the emitted light, resulting in a relatively collimated beam profile.

2.1 Experiments

The fabrication schematics of the GaN-based vertical LED with self-organized nanorod arrays are illustrated in Fig. 1. First, a conventional LED structure was grown on a *c*-plane sapphire substrate by MOCVD. As shown in Fig. 1(a), the epitaxial LED structure consisted of a 30-nm-thick low-temperature grown GaN buffer layer, a 2-μm-thick undoped GaN, and a 2-μm-thick heavily doped n-type GaN, followed by 20 pairs of InGaN–GaN multiple quantum-wells (MQWs) with a total thickness of 0.2 μm, and a 0.2-μm-thick p-type GaN layer. A layer of indium–tin–oxide (ITO) with a thickness of 240 nm was then deposited on p-GaN, followed by the electron-beam deposition of Ti/Al/Ti/Au with a total thickness of 2 μm for adhesion and as a reflective mirror after wafer bonding. Next, as illustrated in Fig. 1(b), the wafer bonding process began with the deposition of bonding metals comprising Cr/Pt/Au of 50/50/2000 nm on both the LED structure and the silicon wafer. These two wafers were immediately placed in contact with each other using a designed fixture to ensure uniform pressure across both wafers, followed by oven annealing at 350 °C for 30 min in the nitrogen ambient. Since silicon has a higher thermal conductivity (1.457 W/cm °C) than that of sapphire (0.35 W/cm °C) at room temperature, the host Si substrate also functions as a heat sink. After wafer-bonding, the sapphire substrate was removed by an LLO process using a KrF excimer laser (Lambda Physick LPX200) at 248-nm wavelength with a pulsewidth of 25 ns; the laser output power and beam spot size were 10 mW and 1×1 mm^2, respectively.[12] The undoped GaN was also removed by ICP-RIE. Subsequently, the mesa with an area of 1×1 mm^2 was defined by using standard photolithography and dry etching, and then passivated with SiN_x. As shown in Fig. 1(c), the fabrication of nanorod arrays employed self-assembled silica nanospheres as the lithographic and etch masks, which provide greater etching selectivity to n-GaN layer than other polymers. The silica spheres were first suspended in deionized (DI) water diluted in a solution of surfactant at a volume ratio of 5:1, and then spin-coated on the n-GaN surface, followed by heating treatment for adhesion. The surfactant can lower the surface tension and then help the particles spread across the GaN surface. The coated sample was then etched by ICP-RIE, using Cl and Ar as the etch gases at a fixed flow rate of 45 and 30 sccm, respectively. The device was immersed in DI water with sonification for 3 min to remove silica particles, followed by surface passivation with silicon dioxide (SiO_2) for electric isolation. Finally, a bonding pad comprised of Cr–Pt–Au was deposited by electron-beam evaporation on the back side of Si substrate. The fabricated GaN–InGaN VI-LEDs is illustrated in Fig. 1(d).

1.

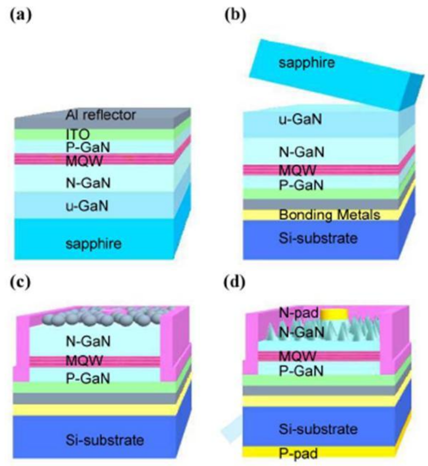

Fig.1. Fabrication schematics of a GaN–InGaN VI-LED with self-organized nanorod arrays: (a) the epitaxial structure, (b) wafer bonding and LLO processes, (c) nanorod fabrication involving self-assembled silica spheres as lithographic and etch masks, and (d) the fabricated device schematic.

2.

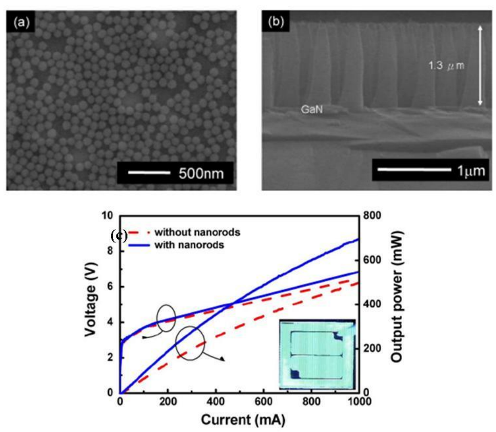

Fig.2. Field-emission scanning-electron micrographs (FE-SEM) of (a) the densely packed silica spheres on GaN, showing a mean diameter of 100 nm with a uniformity of better than 1%; (b) the cross-sectional view of the fabricated nanorods with a base diameter of 200 nm and a height of 1.3 μm, similar to cone structures. (c) voltage and light output intensity versus forward current characteristics for a conventional GaN–InGaN VI- LED without nanorods) and the VI-LEDs with nanorod arrays. The inset shows the uniform light emission from the VI-LEDs with nanorod arrays at a driving current of 350 mA.

3.

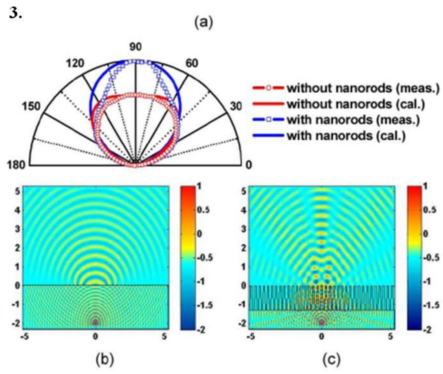

Fig.3. (a) Measured and simulated emission profiles of a GaN–InGaN VI-LEDs with and without nanorod arrays, where the snap shots of simulated wave propagation are shown in (b) and (c), respectively.

2.2 Results and Discussion

Fig. 2(a) shows the field-emission scanning-electron micrograph (SEM) of the spin-coated silica spheres on GaN. The closely packed silica nanospheres have a mean diameter of 100 nm with a uniformity of better than 1%. The cross-sectional SEM image of the fabricated nanorod arrays patterned by silica spheres is shown in Fig. 2(b). These nanorods are vertically aligned to the surface normal of GaN and uniformly distributed over the entire surface. Moreover, the dense nanorod arrays exhibit uniform dimensions with a base diameter of 200 nm and a length of 1.3 μm, which resemble cone structures. Since the dimensions of nanorods are comparable to the emission wavelength, the spatially varied rod profiles can enhance optical transmission by collectively functioning as a gradient index layer, similar to that of a zero-order grating.[13] The enhancement in light extraction is also verified by finite-difference time-domain (FDTD) calculations.

The forward current–voltage (*I–V*) characteristics at room temperature for vertical LEDs with and without nanorod arrays are plotted in Fig. 2(c). The measured forward voltages at an injection current of 350 mA for vertical LEDs with and without nanorod arrays are 4.69 and 4.50V, respectively. The slightly increased forward voltage for the vertical LEDs with nanorod arrays is attributed to the reduced lateral-current spreading on n-GaN, giving rise to a slightly increased resistivity. Nonetheless, both *I–V* curves are nearly identical, indicating the negligible impact of nanorod arrays. Fig. 2(c) also shows the corresponding light output intensity versus forward current (*I–V*) characteristics. At an injection current of 350 mA, the light output power of the vertical LEDs with nanorod arrays is 316 mW, approximately enhanced by 40% compared to that without nanorods, 226 mW. The peak emission wavelength is the same as that of a conventional vertical LEDs, occurring at 465 nm. The inset of Fig. 2(c) demonstrates the uniform illumination from the vertical LEDs with nanorod arrays at a driving current of 350 mA under an optical microscope.

The measured far-field emission profiles are shown in Fig. 3(a) for vertical LEDs with and without nanorod arrays. As seen in Fig. 3(a), the emission from vertical LEDs with high-aspect-ratio nanorods is mainly enhanced along the surface normal view angle of ±30°. The integrated intensity is improved by a factor of 38% within a view angle of 20°. A two-dimensional FDTD method with perfectly matched layer boundary within a condition is employed to investigate the emission characteristics from high-aspect-ratio nanorod arrays. The simulated far-field patterns are plotted in Fig. 3(a) for comparison. Fig. 3(b) and (c) show the snap shots of wave propagating across a GaN–air interface and an interface with nanorod arrays, respectively. The time-varying current-excited radiation source is placed ~2 μm below the GaN–air interface. The dimensions of nanorods are extracted from the SEM picture shown in Fig. 2(b). As shown in Fig. 3(a), a conventional GaN–air interface results in Lambertian-like radiation patterns with a view angle at the full-width at half-maximum of ~120°. The radiation pattern from the nanorod arrays is relatively collimated, ~100°. As shown in Fig. 3(c), the nanorods suppress the total internal reflection at GaN–air interface, effectively reducing the energy confined in GaN slab. The light extraction enhancement is due to similar mechanisms provided by other surface roughness techniques. However, as shown in Fig. 3(c), the nanorods also act as waveguiding channels for the emitted light, resulting in a relatively collimated radiation pattern. Calculations show that the height of nanorods to be at least a few wavelengths long to provide a sufficient guiding effect. Moreover, the closer the nanorod array to MQWs, the better the directionality. However, the distance in this device is limited to ~1 μm, which is optimized for current spreading.

2.3 Conclusion

In summary, the GaN-based vertical LEDs with high-aspect-ratio nanorod arrays are demonstrated by using self-organized silica spheres for patterning, followed by ICP-RIE. The output power of a vertical LED with nanorod arrays is improved by 40% due to enhanced light extraction. Based on the measured far-field profiles, the enhancement is mainly along the surface normal direction, within a view angle of 20°. We believe that vertical LEDs with high-aspect-ratio nanorod arrays offer a viable solution for efficiency enhancement and radiation profile shaping, suitable for applications in solid state lighting and displays.

3. ZNO NANOROD ARRAYS ON VERTICAL LED

In this part, we introduce anthoer structure for further enhancing the light extraction, improving current spreading, as well as an omnidirectional extractor. By synthesizing the ZnO nanorod array in aqueous solution at room temperature and integrating the GaN-based LLO LED n-side surface, a high-efficiency GaN-based vertical LED was achieved. The light output enhanced mechanism is that ZnO nanotips on the GaN-based vertical LEDs provide an omnidirectional extraction surface and a gradually changed effective refractive index.[14] The refractive index of ZnO is very similar to GaN, and the vertically aligned ZnO nanorods grew well on the GaN surface. Hence, the light output of the fabricated GaN-based vertical LED could be further increased. In addition, synthesizing the ZnO nanorods in aqueous solution at room temperature costs much less and is a mass producible technique compared to that grown by MOCVD.

3.1 Experiments

The schematic of the GaN-based vertical LEDs with ZnO nanorod arrays is shown in Fig. 4. Basically, the fabrication process is similar to that introduced in the first part. We followed the vertical LED process to fabricate the high efficiency vertical LED combined with wafer bonding and LLO techniques. After metal deposition and sidewall passivation process, the devices were performed by the ZnO nanorod formation process.

ZnO nanorod arrays were then synthesized on the surface of the GaN-based vertical LED n-side surface to provide an omnidirectional extraction surface and the gradually changed effective refractive index. The 15 nm thick ZnO thin films were first deposited on the n-GaN surface of the vertical LED by radio-frequency magnetron sputtering.[17] Zinc nitrate hexahydrate [$Zn(NO_3)_2 \cdot 6H_2O$] was used as the zinc precursor to synthesize the ZnO nanorod arrays. Methenamine ($C_6H_{12}N_4$), also called hexamethylenetetramine (HMT), is a highly water-soluble, nonionic tetradentate cyclic tertiary amine used to comply simultaneously with the precipitation of the divalent post-transition metal Zn^{2+} ions, the nucleation growth of its stable oxide form, zincite ZnO. An equimolar (0.02 M) aqueous solution of [$Zn(NO_3)_2 \cdot 6H_2O$] and HMT was prepared in a bottle. Subsequently, the GaN-based vertical LED samples were placed inside the aqueous solutions at room temperature with a synthesis time of 5 hr. After that, the GaN-based vertical LED samples were removed from the aqueous solutions, rinsed with distilled water, and dried at room temperature overnight (Fig. 4f). The details of synthesizing the ZnO nanorod arrays can be found in Ref. 18.

4.

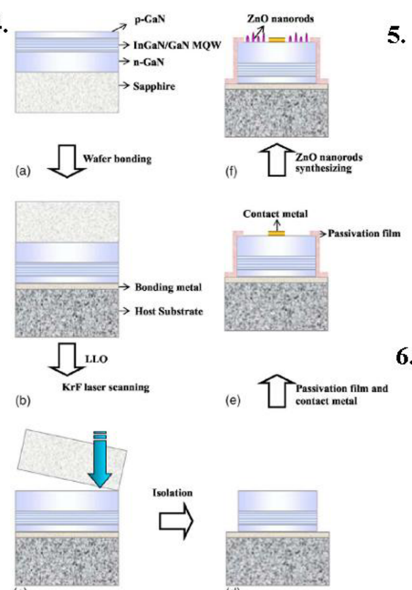

5.

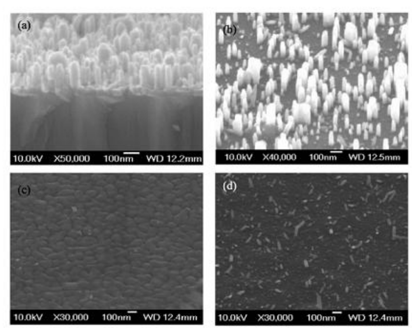

6.

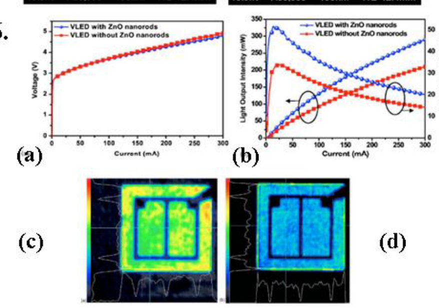

Fig. 4. (Color online) Schematic illustration of the GaN-based vertical LED process flow chart. (a) The GaN-based LED structure. (b) The LED structure was bonded on a host substrate. (c) vertical process by KrF excimer laser. (d) vertical LED isolation process by ICP etching. (e) Deposit SiO_2 passivation film by PECVD and contact metal by E-gun. (f) Synthesized ZnO nanorods in aqueous solution at room temperature.

Fig 5. FESEM images of the GaNbased LEDs with ZnO nanorod arrays: (a) cross-sectional image of the synthesized ZnO nanorod arrays, (b) images of the n-GaN surface, (c) images of the bonding pad metal surface, and □d□ images of the passivation SiO_2 surface.

Fig. 6. (a) I-V and (b) L-I and WPE vs forward dc current for the GaN-based vertical LED with ZnO nanorod arrays and that without ZnO nanorod arrays fabricated in this letter. Intensity distribution pattern of the GaN-based vertical LEDs (c) with and (d) without a ZnO nanorod array omnidirectional extraction surface at a driving current of 200 mA.

3.2 Results and Discussion

The SEM pictures of the GaN-based vertical LEDs with ZnO nanorod arrays synthesized in aqueous solutions at room temperature are shown in Fig. 5. Figure 5a shows the cross-sectional image of the synthesized ZnO nanorod arrays with dimensions of 30–90 nm in diameter and 100–300 nm in length, respectively. The random-sized ZnO nanorod arrays not only provide an omnidirectional extraction surface but a layer with a gradually changing refractive index, which could increase the probabilities for light extraction. According to our previous work, the dimensions of the synthesized ZnO nanorod arrays could be controlled by the concentration of the aqueous solution and the growth time. The SEM images of the ZnO nanorod arrays on different surfaces, n-GaN, contact metal, and passivated SiO_2 film, are shown in Fig. 5 (b) to (d). The well-aligned high density, about 1.5×10^{10} cm^{-2}, of the synthesized ZnO nanorod arrays on the n-GaN surface is shown in Fig. 5(b). The growth direction of the synthesized ZnO nanorod arrays on the n-GaN surface is perpendicular to the n-GaN surface. In contrast to the n-GaN surface, there were nearly no ZnO nanorod arrays synthesized on the metal surface, as shown in Fig. 5c. Figure 5d shows the SEM images of the passivated SiO_2 surface and a lower density, about 4×10^9 cm^{-2}, of ZnO nanorod arrays could be observed. This observation strongly reveals the importance of surface characterization on the growth behavior of the ZnO nanorods in the aqueous solution.

Fig. 6 (a) shows the forward current–voltage (*I-V*) curves for the GaN-based vertical LED with ZnO nanorod arrays and that without ZnO nanorod arrays. It was found that the measured forward voltages under 200 mA injection currents at room temperature for the GaN-based vertical LED with ZnO nanorod arrays and that without ZnO nanorod arrays were approximately 4.26 and 4.33 V, respectively. The slightly lower forward voltage of the LED with ZnO nanorod arrays than that without ZnO nanorod arrays could be attributed to the current spreading layer of the synthesized ZnO layer on the surface. Fig. 6 (b) shows that the light-output intensity and the wall-plug efficiency (WPE) vs forward dc current for the GaN-based vertical LED with ZnO nanorod arrays and that without ZnO nanorod arrays are taken as continuous-wave. At an injection current of 200 mA, the light-output powers of the GaN-based vertical LED with ZnO nanorod arrays and that without ZnO nanorod arrays were approximately 220 and 158 mW, respectively. The emission wavelength of the GaN-based vertical LEDs with and without ZnO nanorods were both at 460 nm. The GaN-based vertical LED with ZnO nanorod arrays increased the output power intensity by a factor of 1.39, indicating that ZnO nanorod arrays provided an omnidirectional extraction surface with a gradually changing refractive index and had better light extraction efficiency than that without ZnO nanorod arrays. The WPE varies in a similar manner as the output power with forward dc current. The WPE of the GaN-based vertical LED with ZnO nanorod arrays is 1.41 times higher than that without ZnO nanorods under all our measurement conditions. According to Fig. 6b, at a driving current of 200 mA, the WPE values for the GaN-based vertical LED, with and without ZnO nanorod arrays, were 25.8 and 18.3%, respectively.

To further investigate the influence of the omnidirectional extraction surface by ZnO nanorod arrays on light output performance of the GaN-based vertical LEDs, intensity distribution measurements were performed on that with and without ZnO nanorod arrays. Fig. 6 (c) and (d) shows the photos of the GaN-based vertical LEDs, with and without ZnO nanorod arrays, with injecting a 200 mA dc current in these two different devices, respectively. Each intensity distribution is also shown in the same figure. The electroluminescence intensities observed from GaN-based vertical LEDs with ZnO nanorod arrays were obviously greater than those observed from that without ZnO nanorod arrays at the same injection current at the top surface area. Such an enhancement could be attributed to the omnidirectional extraction surface by ZnO nanorod arrays allowing photons to have a larger probability of being emitted from the device in the top emission direction, thus achieving even brighter LEDs.

3.3 Conclusion

In summary, a simple and novel method to enhance the light output of the GaN-based vertical LED by synthesizing ZnO nanorod arrays on the surface was investigated. The coated ZnO thin layer and the synthesized ZnO nanorod arrays were applied to GaN-based vertical LEDs to increase their extraction efficiency. The growth of the synthesized ZnO nanorod arrays was strongly dependant on the surface characteristics. The formation of the ZnO nanorod arrays on the GaN-based LLO LED surface increased the light output power and WPE up to 220 mW and 26%, which were increased by 38.9 and 41.2%, respectively, when compared to that without ZnO nanorod arrays at a driving current of 200 mA and with a chip size of 700 μm × 700 μm. Such an omnidirectional extraction surface with ZnO nanorod arrays could mainly enhance the light output intensity due to the improvement of the escape probability of photons inside the GaN-based LLO LED structure.

4. LED REGROWTH ON A SIO_2 NANOROD-ARRAY PATTERNED SAPPHIRE SUBSTRATE

As mentioned in previous part, the LEDs grown on the nanoscale PSS showed more enhancement in the EQE than those grown on the microscale PSS. However, the fabrication of nanoscale PSSs generally required electron-beam lithography[19] or nanoimprinting techniques,[20] making it unfavorable for mass production. In this letter, we report a relatively simple technique to fabricate a SiO_2 nanorod-array PSS (NAPSS), serving as a template for the nanoscale ELO (NELO) of GaN by MOCVD to produce high efficiency GaN-based LEDs. The transmission electron microscopy (TEM) images showed that the TDD was significantly reduced by the voids between SiO_2 nanorods and the stacking faults introduced during the NELO. Moreover, the NAPSS LEDs demonstrated an enhanced EQE and light-output power compared to a conventional LED epitaxially grown on a flat sapphire substrate.

4.1 Experiments

The GaN-based LEDs used in this study were grown on a 2 inch SiO_2 NAPSS using a low-pressure MOCVD system (Aixtron 2400 G). The preparation of the SiO_2 NAPSS template started with the deposition of a 200-nm-thick SiO_2 layer on a c-face (0001) sapphire substrate by plasma enhanced chemical vapor deposition, followed by the evaporation of a 10-nm-thick Ni layer, and the subsequent rapid thermal annealing with a flowing nitrogen gas at 850 °C for 1 min. The resulting self-assembled Ni clusters then served as the etch masks to form a SiO_2 nanorod array using a reactive ion etch system for 3 min. Finally, the sample was dipped into a heated nitric acid solution (HNO_3) at 100 °C for 5 min to remove the residual Ni masks. As shown in Fig. 7(a), the field-emission scanning electron micrograph (FESEM) indicated that the fabricated SiO_2 nanorods were approximately 100–150 nm in diameter with a density of 3×10^9 cm^{-2}. The spacing between nanorods was about 100–200 nm. Fig. 7(a) also shows that the exposed sapphire surface was flat enough for epitaxy. As the deposition process began, localized and hexagonal islandlike GaN nuclei were first formed from the sapphire surface to initiate GaN overgrowth, as shown in Fig. 7(b). Fig. 7(c) shows the cross-sectional FESEM image of the GaN epilayer, where voids with a size varying from 150 to 200 nm were observed between the highlighted SiO_2 nanorods. The existing of the voids between nanorods observed from the micrographs suggested that not all the exposed surface enjoyed the same growth rate. Hence, only the regions with higher growth rates, which might be originated from larger exposed surface, could play the role of a seed layer, facilitating the lateral coalescence of GaN. Lastly, the growth of a conventional LED structure, which consists of ten periods of InGaN/GaN multiple quantum wells and a 100-nm-thick p-GaN layer, was completed by MOCVD. The p-GaN layer of the NAPSS LED was grown at the relatively low temperature of 800 °C, leading to the formation of hexagonal pits due to insufficient migration length of Ga atoms.[21] The FESEM image of the roughened p-GaN surface with randomly distributed pits is shown in Fig. 7(d).

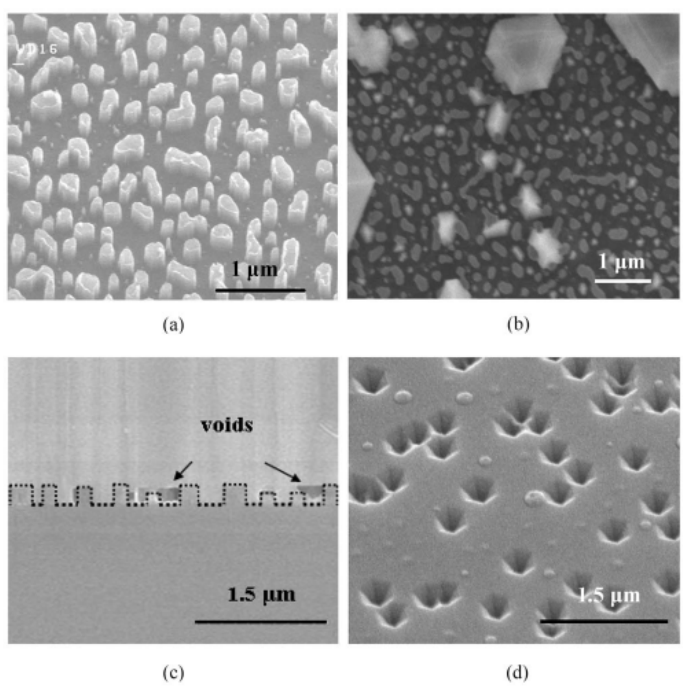

Fig. 7. FESEMs of (a) the fabricated SiO_2 nanorod array, (b) GaN nuclei on the SiO_2 NAPSS as growth seeds, (c) the GaN epilayer on a NAPSS in the cross-sectional view, and (d) the epitaxial pits on the p-GaN surface.

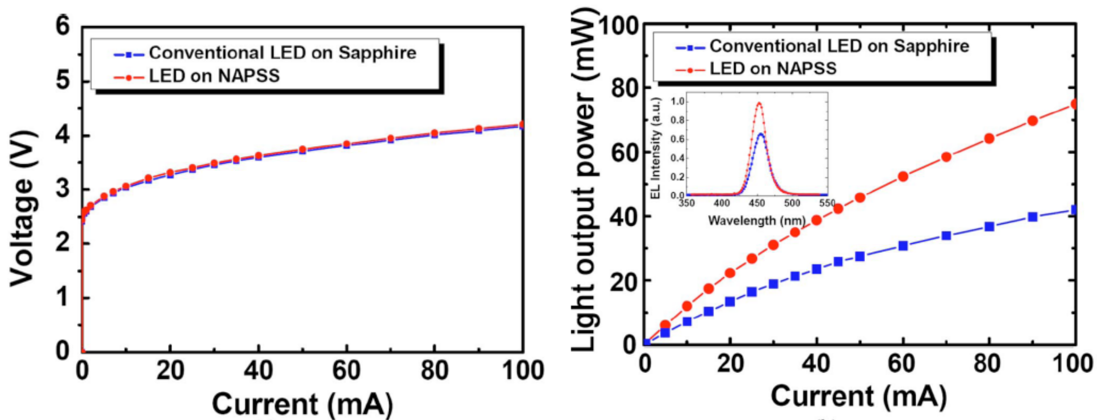

(a) (b)

Fig. 8. Electrical and optical properties of a NAPSS and a conventional LED: (a) the current-voltage (I-V) curves, and (b) the current-output power (L-I) curves, where the inset shows the electroluminescence spectra for both devices at a driving current of 20 mA.

4.2 Results and Discussion

The completed epitaxial structure then underwent a standard four-mask LED fabrication process with a chip size of 350 × 350 μm^2 and packaged into TO-18 with epoxy resin on top. The schematic of a fabricated NAPSS LED is shown in the inset of Fig. 8(a). The current-voltage (*I-V*) characteristics of the NAPSS LED and a conventional LED with the same chip size were measured at room temperature, as shown in Fig. 8(a). The forward voltages at 20 mA were 3.27 V for the conventional LED and 3.31 V for the NAPSS LED. The nearly identical I-V curves indicate that the nanoscale roughness on the p-GaN surface had little impact on the I-V characteristics. Moreover, the NELO of GaN did not deteriorate the electrical properties. Figure 10(b) shows the measured light-output power versus the forward continuous dc current (*L-I*) for the NAPSS and conventional LED. At an injection current of 20 mA, the light-output powers were approximately 22 and 14 mW for the NAPSS and the conventional LEDs, respectively. The output power of the NAPSS LED was enhanced by a factor of 52% compared to that of the conventional LED. The inset shows the normalized electroluminescence spectra for both devices at an injection current of 20 mA. A minor wavelength blueshift of ~2 nm was observed for the NAPSS LED, attributed to the partial strain release by adopting the NELO scheme.[26] The EQE of the NAPSS LED was calculated to be ~40.2%, which is an increase of 56% when compared to that of the conventional LED, ~25.7%. We believe that the 56% enhancement in EQE originated from the improved internal quantum efficiency and the enhanced extraction efficiency. The SiO_2 NAPSS-assisted NELO method effectively suppressed the dislocation densities of GaN-based LEDs, which increased the internal quantum efficiency. Moreover, the embedded SiO_2 nanorods in the GaN epilayer contributed to light extraction due to scattering at the interfaces of different refractive indices. Ueda et al.[27] reported that the output power linearly increased with the surface coverage ratio of nanosilica spheres. Therefore, the extraction efficiency was enhanced by the SiO_2 nanorod array.

4.3 Conclusion

In summary, this work introduced the SiO_2 NAPSS-assisted NELO method suitable for the MOCVD growth of the next-generation high-brightness blue LEDs. The NAPSS LED demonstrated an enhanced EQE and light-output power when compared to a conventional LED. The TDD reduction in GaN-based epilayers was realized by the SiO_2 NAPSS-assisted NELO method, where four potential TD reduction mechanisms were identified.

5. SUMMARY

We have demonstrated high efficiency GaN-based LEDs by fabricating GaN, ZnO nanorods on the surface of vertical LED and regrowth on SiO_2 nanorod NPSS. Vertical LEDs with GaN and ZnO nanorod enjoy better light extraction efficiency than that without nano structures on the surface by destroying total internal reflection at the surface. These nano structures not only benefit to the light extraction but also contribute to better directionality. Besides, regrowth GaN-based LED on SiO_2 NAPSS could effectively improve the extraction efficiency and suppress the dislocation formation simultaneously.

REFERENCES

[1] S. Nakamura and G. Fasol, The Blue Laser Diode, Springer, New York (1997).

[2] H. W. Huang, C. C. Kao, J. T. Chu, H. C. Kuo, S. C. Wang, and C. C. Yu, IEEE Photon. Technol. Lett., 17, 983 (2005).

[3] C. C. Kao, H. C. Kuo, H. W. Huang, J. T. Chu, Y. C. Peng, Y. L. Hsieh, C. Y. Luo, S. C. Wang, C. C. Yu, and C. F. Lin, IEEE Photon. Technol. Lett., 17, 19 (2005).

[4] T. Fujii, Y. Gao, R. Sharma, E. L. Hu, S. P. DenBaars, and S. Nakamura, Appl. Phys. Lett., 84, 855 (2004).

[5] J. K. Kim, H. Luo, Y. Xi, J. M. Shah, T. Gessmann, and E. F. Schubert, J. Electrochem. Soc., 153, G105 (2006).

[6] A. Sakai, H. Sunakawa, and A. Usui, Appl. Phys. Lett. 71, 2259 (1997).

[7] D. S. Wuu, W. K. Wang, K. S. Wen, S. C. Huang, S. H. Lin, R. H. Horng, Y. S. Yu, and M. H. Pan, J. Electrochem. Soc. 153, G765 (2006).

[8] H. Gao, F. Yan, Y. Zhang, J. Li, Y. Zeng, and G. Wang, J. Appl. Phys. 103, 014314 (2008).

[9] M. Y. Hsieh, C. Y. Wang, L. Y. Chen, T. P. Lin, M. Y. Ke, Y. W. Cheng, Y. C. Yu, C. P. Chen, D. M. Yeh, C. F. Lu, . F. Huang, C. C. Yang, and J. J. Huang, IEEE Electron. Device Lett., vol. 29, no. 7, pp. 658–660, Jul. (2008).

[10] D. H. Kim, C. O. Cho, Y. G. Roh, H. Jeon, Y. S. Park, J. Cho, J. S. Im, C. Sone, Y. Park, W. J. Choi, and Q. H. Park, Appl. Phys. Lett., vol. 87, pp. 203508–1, (2005).

[11] C. H. Chiu, C. E. Lee, C. L. Chao, B. S. Cheng, H. W. Huang, H. C. Kuo, T. C. Lu, S. C. Wang, W. L. Kuo, C. S. Hsiao, and S. Y. Chen, Electrochem. Solid-State Lett., vol. 11, pp. H84–H87, (2008).

[12] J. T. Chu, T. C. Lu, H. H. Yao, C. C. Kao, W. D. Liang, J. Y. Tsai, H. C. Kuo, and S. C. Wang, J. Appl. Phys., vol. V45, no. 4A, pp. 2556–2560, (2006).

[13] Y. F. Huang, S. Chattopadhyay, Y. J. Jen, C. Y. Peng, T. A. Liu, Y. K. Hsu, C. L. Pan, H. C. Lo, C. H. Hsu, Y. H. Chang, C. S. Lee, K. H. Chen, and L. C. Chen, Nature Nanotech., vol. 2, pp. 770–774, (2007).

[14] J. Zhong, H. Chen, G. Saraf, Y. Lu, C. K. Choi, J. J. Song, D. M. Mackie, and H. Shen, Appl. Phys. Lett., 90, 203515 (2007).

[15] H. R. Shanks, P. D. Maycock, P. H. Sidles, and G. C. Danielson, Phys. Rev., 130, 1743 (1963).

[16] C. F. Chu, F. I. Lai, J. T. Chu, C. C. Yu, C. F. Lin, H. C. Kuo, and S. C. Wang, J. Appl. Phys., 95, 3916 (2004).

[17] C. C. Lin, C. S. Hsiao, S. Y. Chen, and S. Y. Cheng, J. Electrochem. Soc., 151, G285 (2004).

[18] S. C. Liou, C. S. Hsiao, and S. Y. Chen, J. Cryst. Growth, 274, 438 (2005).

[19] A. Xing, M. Davanco, D. J. Blumenthal, and E. L. Hu, J. Vac. Sci. Technol. B 22, 70 (2004).

[20] H. W. Huang, C. H. Lin, C. C. Yu, B. D. Lee, C. H. Chiu, C. F. Lai, H. C. Kuo, K. M. Leung, T. C. Lu, and S. C. Wang, Nanotechnology 19, 185301 (2008).

[21] Y. J. Lee, H. C. Kuo, T. C. Lu, and S. C. Wang, IEEE J. Quantum Electron. 42, 1196 (2006).